Interstrand Cross-Linking by Bizelesin Produces a Watson–Crick to Hoogsteen Base-Pairing Transition Region in d(CGTAATTACG)$_2$†

Frederick C. Seaman* and Laurence Hurley*

Drug Dynamics Institute, College of Pharmacy, The University of Texas at Austin, Austin, Texas 78712

Received June 30, 1993; Revised Manuscript Received September 29, 1993®

ABSTRACT: ^{1}H NMR analysis of the bizelesin adduct of d(CGTAATTACG)$_2$ indicates that adenines six base pairs apart on opposite DNA strands are cross-linked, yielding two major adduct conformations differing in the central duplex region (5′AATT-3′): one (major product) contains an AT step wherein both adenines are *syn*-oriented and Hoogsteen base paired to thymines (*5HG* model); the other contains *anti*-oriented AT-step adenines that show no evidence of hydrogen bonding with pairing thymines (*5OP* model). The *5OP* model consists of three conformers undergoing exchange and differing in the orientation of the AT-step thymines. Bizelesin's size, rigidity, and cross-linking properties restrict the DNA adduct's range of motion and freeze out DNA conformation(s) adopted during the cross-linking process. This most reactive DNA sequence, 5′-TAATTA-3′, yields an adduct conformation (*5HG*) containing a stable region of Watson–Crick (WC) to Hoogsteen (HG) to Watson–Crick base-pairing transitions. While bizelesin exercises a selective effect on DNA conformation, it intrudes into regions of base stacking less than other Hoogsteen pairing-inducing drugs (e.g., echinomycin). Because of this capacity to induce stable Hoogsteen base pairing with only minimal distortion of base–base stacking, bizelesin affords an opportunity to explore this unusual DNA conformation.

Bizelesin (formerly U77779, The Upjohn Co.), a bifunctional DNA cross-linking antineoplastic agent, consists of two open-ring homologs of the (+)-CC-1065 cyclopropa[*c*]pyrrolo-[3,2-*e*]indol-4(5*H*)-one (CPI)[1] subunit connected by a rigid linker moiety (Figure 1a; Mitchell et al., 1991). It belongs to a class of rigid CPI cross-linking reagents characterized by a right-handed twist approximating DNA minor groove geometry. Bizelesin forms interstrand cross-links through N3 of adenine (Figure 1b) spaced six base pairs apart (inclusive of the adenines) while occupying the intervening minor groove (Mitchell et al., 1991; Ding & Hurley, 1991; Sun & Hurley, 1993). Results from NOESY and ROESY experiments[2] conducted on the self-complementary oligomer (10-mer) 5′-CGTAATTACG-3′ and its bizelesin reaction product are evaluated in order to determine how the B-form 10-mer adjusts to the introduction of the drug.

The findings of the present study indicate that two major conformers comprise the cross-linked reaction products. Each of two independent sets of NMR signals (Tables I and II) corresponds to a duplex adduct conformation, one with the AT-step adenines *syn*-oriented and Hoogsteen base paired to thymines (*5HG* model) and a second with the AT-step adenines *anti*-oriented and paired (but not evidently hydrogen bonded) with thymines displaying extraordinary motion (*5OP* model). As (1) no NOESY or ROESY cross-peaks link the two sets of NMR signals and (2) each set is sufficient to characterize a C_2-symmetrical DNA adduct, *5HG* and *5OP* represent conformationally distinct products of cross-linkage. Although conformational exchange between the *5HG* and *5OP* conformers is undetectable on the NMR time scale, open AT-step base pairing resembling that of the *5OP* model must precede any reorientation of the AT-step adenines resulting in the *5HG* product.

EXPERIMENTAL PROCEDURES

Chemicals. Bizelesin was a gift from The Upjohn Co. Reagents used to prepare the NMR buffer, sodium phosphate (99.99%) and sodium chloride (99.99%), were purchased from Aldrich. HPLC water and methanol were purchased from Baxter Scientific and Fisher, respectively.

Oligonucleotide Preparation and Purification. The self-complementary 10-mer d(CGTAATTACG)$_2$ was synthesized on a 10-μmol scale by using automated solid-phase phosphotriester and phosphoramidite chemistry (Gait, 1984) on an Applied Biosystems automated DNA synthesizer (model 381A). It was purified on a Machery-Nagel Nucleogen-DEAE 60-7 HPLC column with an increasing gradient to 1 M NaCl in 15 mM sodium phosphate and 20% acetonitrile/aqueous buffer, pH 6.8.

Adduct Preparation and Purification. The bizelesin adduct was prepared by stirring 15 mg of bizelesin in 0.2 mL of DMF solution with 0.03 mL of aqueous sodium bicarbonate for 20 min before adding 40 mg of purified 10-mer in 0.75 mL of buffer containing 20 mM sodium phosphate and 200 mM sodium chloride. The reaction mixture was stirred for 4 days in the dark, lyophilized to dryness overnight, desalted and separated from excess drug on C_{18} Sep-Pak cartridges (Waters), and purified using HPLC conditions, as described above. *5HG* and *5OP* conformers were inseparable by HPLC.

Proton NMR Experiments. One- and two-dimensional 500-MHz ^{1}H and 202.44-MHz ^{31}P NMR data sets in buffered

† This research was supported by grants from the U.S. Public Health Service (CA-49751), the Welch Foundation, The Upjohn Co., and the Burroughs Wellcome Scholars Program.

* Address correspondence to either author.

® Abstract published in *Advance ACS Abstracts,* November 1, 1993.

[1] Abbreviations: NMR, nuclear magnetic resonance; NOE, nuclear Overhauser effect; 2QF-COSY, double-quantum-filtered correlated spectroscopy; ROESY, rotating frame Overhauser spectroscopy; ^{1}H–^{31}P COSY, hydrogen–phosphorus correlated spectroscopy; ppm, parts per million; FID, free induction decay; DEAE, diethylaminoethyl; DMF, dimethylformamide; WC, Watson–Crick base pairing; HG, Hoogsteen base pairing; OP, open base pairing; CPI, cyclopropa[*c*]pyrrolo[3,2-*e*]-indol-4(5*H*)-one.

[2] Data from other NMR experiments (e.g., 2QF-COSY and ^{1}H–^{31}P COSY) are currently being evaluated to further refine the bizelesin adduct structures presented here.

0006-2960/93/0432-12577$04.00/0

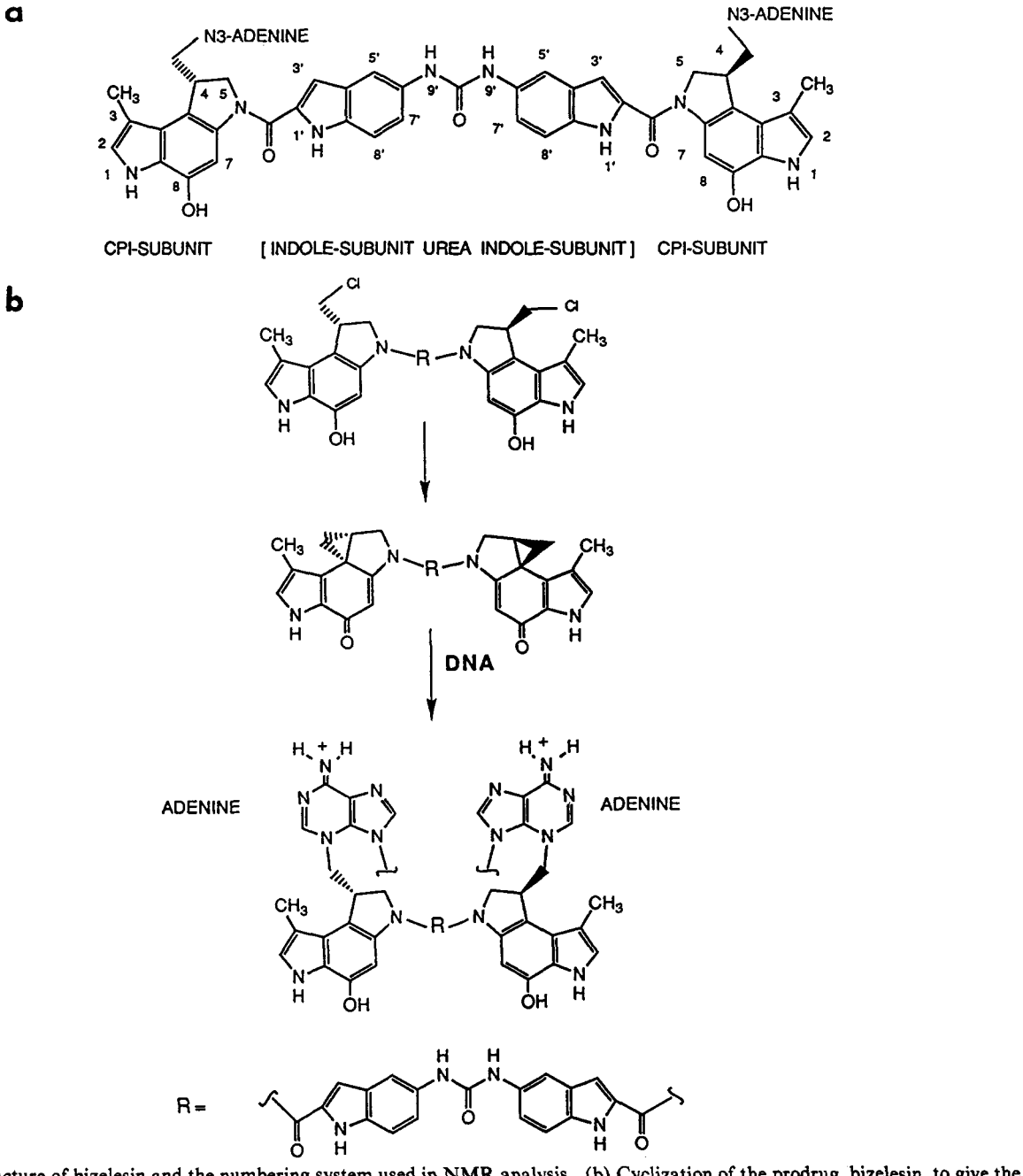

FIGURE 1: (a) Structure of bizelesin and the numbering system used in NMR analysis. (b) Cyclization of the prodrug, bizelesin, to give the cyclopropyl derivative followed by the reaction of adenines of opposite DNA strands to form the cross-linked adduct.

H_2O and D_2O solutions were recorded on General Electric GN-500 and Bruker AMX 500 FT NMR spectrometers. Proton chemical shifts were recorded in parts per million (ppm) and referenced relative to external TSP (1 mg/mL) in D_2O (HOD signal was set to 4.751 ppm). Phosphorus chemical shifts were referenced relative to external 85% H_3PO_4 in D_2O.

Phase-sensitive two-dimensional NOESY spectra (Bruker) were obtained for two mixing times: 100 and 200 ms. All spectra were acquired with 16 scans at each of 1024 t_1 values, a spectral width of 10.002 ppm, and a repetition time of 10 s between scans. During data processing, a shifted squared sine-bell function (shift = 45°) was used in both w_1 and w_2 dimensions. The FID in w_1 was zero-filled to 2K prior to Fourier transformation to give a 2K × 2K spectrum. 2D NOE spectra in 90% H_2O at 150-ms mixing time were recorded using the 1–1 echo read pulse sequence (Sklenar & Bax, 1987; Blake & Summer, 1990) with a 2.5-s pulse repetition time, a sweep width of 24.396 ppm, and a 90° pulse width of 28.75 ms.

Exchange processes were studied by ROESY (Bothner-By et al., 1984) in D_2O with a spectral width of 5000 Hz in both dimensions. Mixing times of 100 and 200 ms were used to collect 512 FIDs, each of 32 scans, and to generate 2 × 512 × 1024 data matrices.

Restrained Molecular Dynamics. Interproton distances were derived via the program MARDIGRAS (Borgias & James, 1989, 1990) from NOESY experiments involving mixing times of 100 and 200 ms. A complete 2D NOE relaxation matrix was set up using the geometry of a starting structure to provide interproton NOEs not available from the experimental data sets. Alternative starting structures were (1) the bizelesin 10-mer adduct nonrestrained molecular dynamics product and (2) the minimized B-DNA adduct. The complete NOE matrix was calculated for the starting

Table I: Chemical Shifts of Nonexchangeable and Exchangeable Protons of the 5-Adenine *Syn*-Oriented Model (*5HG*) and the 5-Adenine Open Model (*5OP*)

	H1′		H2′		H2″		H3′		H4′		H5′		H5″		PuH8/PyH6		TMe/CH5/AH2		PuH1/PyH3	
base	*5HG*	*5OP*	*5HG*	*5OP*	*5HG*	*5OP*	*5HG*	*5OP*	*5HG*	*5OP*	*5HG*	*5OP*	*5HG*	*5OP*	*5HG*	*5OP*	*5HG*	*5OP*	*5HG*	*5OP*
C	5.57	5.68	1.81	1.81	2.30	2.29	4.65	4.67	4.02	4.04	3.64	3.64	3.64	3.64	7.54	7.54	5.78	5.78		
G	5.90	5.82	2.58	2.57	2.64	2.58	4.95	4.96	4.31	4.30	4.07	4.07	3.93	3.92	7.90	7.91			12.53	12.51
T	5.64	5.69	2.20	2.28	2.52	2.57	4.91	4.93	4.27	4.29	4.18	4.17	4.12	4.09	7.32	7.39	1.69	1.70	11.14	11.39
A	6.06	6.06	2.58	2.63	3.00	2.81	4.83	4.91	4.03	4.09	4.18	4.30	4.11	4.22	8.24	8.30	7.36	6.96		
A	5.27	6.08	2.88	2.30	2.35	2.47	4.58	4.67	3.40	3.37	3.22	3.28	3.07	2.61	7.48	7.92	7.59	7.36		
T	5.78	5.50	2.00	1.52	2.49	2.28	4.51	4.35	1.99	1.38	3.24	3.35	3.24	2.48	6.75	(a)[a] 6.62 (b) 6.33 (c) 6.77	0.60	(a) 1.09 (b) 0.88 (c) 0.70	12.38	NO[b]
T	5.23	5.24	1.96	1.88	1.98	1.97	4.56	4.62	2.49	3.39	3.95	4.00	3.90	3.78	7.32	7.12	1.52	(a) 1.40 (b) 1.49 (c) 1.41	14.68	14.23
A	5.86	5.89	2.78	2.68	2.60	2.72	4.89	4.89	4.20	4.22	3.79	3.88	2.57	2.68	8.45	8.38	8.23	8.10		
C	5.33	5.33	1.77	1.76	2.13	2.12	4.60	4.60	2.27	2.25	3.76	3.79	3.29	3.39	7.32	7.31	5.52	5.52		
G	6.10	6.10	2.62	2.62	2.32	2.32	4.69	4.68	4.23	4.23	4.08	4.08	3.83	3.83	7.85	7.84				

[a] Designations (a), (b), and (c) indicate the chemical shifts of the different 16T positional isomers a, b, and c. [b] NO indicates that the signal is not observed.

Table II: Bizelesin Adduct Drug Chemical Shifts for the *5HG* and *5OP*

	H2	H3Me	NH1	H4a	H4A	H4B	H5A	H5B	H7	H3′	H5′	H7′	H8′	NH1′	NH9′
5HG	7.29	2.59	10.28	4.43	4.62	5.01	4.44	5.30	7.84	7.22	7.45	8.07	7.60	11.33	8.64
5OP	7.29	2.59	10.28	4.60	4.59	5.10	4.59	5.23	7.84	7.75	8.28	8.02	7.56	11.14	7.66

structure using CORMA (Borgias et al., 1987, 1989; Borgias & James, 1988). MARDIGRAS calculates upper and lower bounds for the interproton distances (Borgias & James, 1990). Subsequent procedures followed those described previously (Kerwood et al., 1991).

Interproton distances were incorporated into the constrained molecular dynamics calculations (rMD) of the solvated system. rMD calculations were performed using the SANDER module of AMBER, version 4.0, on an SGI 4D35G Personal Iris workstation (Pearlman, 1991). The AMBER force-field pseudo-energy terms for the interproton distances have the form of flat wells with parabolic sides within a defined distance.

RESULTS

General Strategy for ^1H NMR Assignment of the Two Cross-Linked Adducts. *5HG* and *5OP* NMR signals[3] were assigned following characterization of two ^1H NOESY cross-connectivity networks. In each cross-connectivity network, PyH6/PuH8 protons are linked to each other and to sugar H1′, H2″, H2′, and H3′ and, by extending the internal sugar connectivity via H3′ and H4′, to sugar H5′ and H5″. Adenine H2 substituents and neighboring thymine H3 protons are incorporated into this network through H2 cross-peaks with minor groove sugar H1′. Bizelesin's ^1H substituents are incorporated into the network via their cross-peaks with minor groove duplex protons. All NOESY cross-peaks are assigned to a network, and the total conformational array of reaction products is determined from the number of independent cross-connectivity networks. Finally, spectral evidence confirms conformational exchange between interconverting positional isomers within the *5OP* network (Choe et al., 1991).

Bizelesin Is Attached through N3 of Adenine at 8A (5HG) and 18A (5OP). The *5HG* 8A $H6_b$ and 8A $H6_e$ amino signals (9.11 and 8.52 ppm, respectively) resemble a (+)-CC-1065 adduct's covalently modified adenine $H6_b$ and $H6_e$ in chemical shifts (9.19 and 9.08 ppm) and in their NOESY cross-peaks with the imino proton of the pairing thymine, 3T H3 (Figure 2, H1 and H2), and with each other (Lin et al., 1991). A similar pattern exists for a second set of amino signals, 18A $H6_b$ and 18A $H6_e$, at 8.92 and 8.60 ppm (Figure 2, F1 and F2). As in the (+)-CC-1065 adduct, the downfield shift of the two sets of amino signals from the usual adenine amino signal range (6.0–8.0 ppm) and the upfield shift of the pairing thymine H3 relative to the unmodified duplex (3T H3, difference = 2.34 ppm; 13T H3, difference = 2.09 ppm) are caused by drug attachment at adenine N3.

A Pair of Self-Complementary Aromatic PyH6/PuH8 to H1′ Walks Differing Only in the Central Region of the Duplex Represents the Two Bizelesin 10-mer Duplex Adducts. Cross-connectivity between base protons and the H1′ of the attached sugar (internal) and the sugar H1′ of the 5′-neighboring nucleotide (external) permits a "walk" through the network of internal and external connectivities extending the length of 5′-CGTAATTACG-3′. In contrast to the single walk (not shown) of the unmodified 10-mer spectrum (a single walk is attributable to the C_2 symmetry of the duplex), two different walks can be traced in the NOESY aromatic base/sugar H1′ region of the bizelesin adduct mixture spectrum (Figure 3). The two walks overlap near the periphery but diverge radically at the duplex center. This divergence is maximally expressed by the far-upfield shift of 5A H1′ relative to 15A H1′ (0.81 ppm difference). Further, the 1C → 10G walk pattern differs from that of the 11C → 20G walk by the former's lack of a 5A H8 × 4A H1′ cross-peak, an intense 5A H8 × 5A H1′ cross-peak, and a weak 5A H8 × 6T H1′ cross-peak consistent with 5A *syn* orientation.

Syn Orientation for the 5HG AT-Step Adenines Is Revealed by the Five Adenine H2 and H8 Cross-Peaks. *Syn* orientation

[3] The multiplicity of NMR signals is dealt with by assigning different number systems to the two independent 5′-(CGTAATTACG)$_2$-3′ sets of signals, 1C through 10G and 11C through 20G, corresponding to the *5HG* and *5OP* models, respectively. Symmetry permits each numbering system to be applied to both duplex strands. Distinct conformational exchange signals are differentiated with a, b, and c suffixes (e.g., 16T H6a and 16T H6b). Drug proton signals (Figure 1a) associated with the 5′-1C–10G-3′ sequence begin with the number of the covalently modified adenine base, 8 (e.g., 8H3′). A separate set of drug signals showing connectivity to the 5′-11C–20G-3′ sequence likewise begins with the number of the covalently modified adenine, 18 (e.g., 18H3′). Difficulty in unambiguously assigning deoxyribose H5″ and H5′ led to the designation of the downfield member of the pair as H5′.

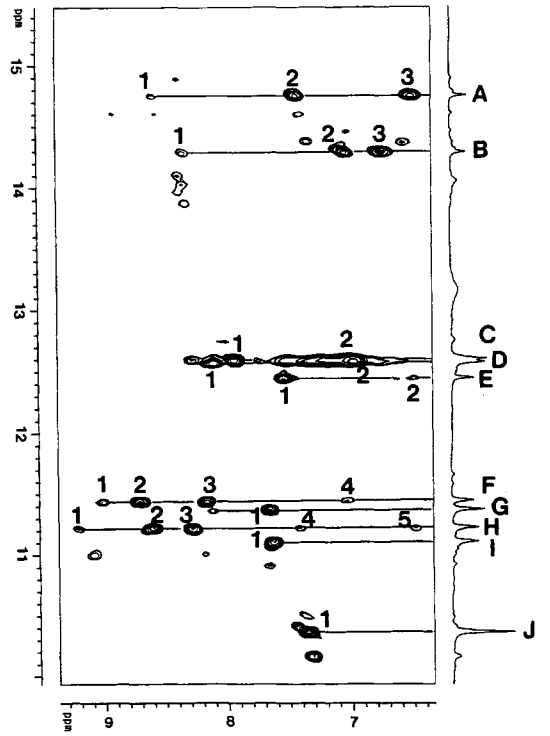

FIGURE 2: Two-dimensional NOESY (150-ms mixing time) expanded contour plot of the bizelesin 10-mer duplex adduct (90% H_2O/10% D_2O) showing the cross-peaks of (1) the G H1 and T H3 imino protons and (2) bizelesin exchangeable ^1H substituents: A, 7T H3 (4A-7T) (1) 8A $H6_e$, (2) 4A H2, (3) 4A $H6_{b,e}$; B, 17T H3 (14A-17T) (1) 18H5′, (2) 14A H2, (3) 14A $H6_{b,e}$; C, 2G H1 (2G-9C) (1) 9C $H4_b$, (2) 9C $H4_e$; D, 12G H1 (12G-19C) (1) 19C $H4_b$, (2) 19C $H4_e$; E, 6T H3 (5A-6T) (1) 5A H8, (2) 4A $H6_{b,e}$; F, 13T H3 (13T-18A) (1) 18A $H6_b$, (2) 18A $H6_e$, (3) 18A H2, (4) 14A H2; G, 8NH1′ (1) 8H8′; H, 3T H3 (3T-8A) (1) 8A $H6_b$, (2) 8a $H6_e$, (3) 8A H2, (4) 4A H2, (5) 4A $H6_{b,e}$; I, 18NH1′ (1) 18H8′; J, 8/18NH1 (1) 8/18H2.

requires that *5HG* 5A H2 project deeply into the major groove and H8 extend shallowly into the minor groove. 5A H2 cross-peaks with 4A H8 (Figure 4a, cross-peak 1), 4A H2″ and H2′ (Figure 4c, cross-peaks 10 and 11), 4A H3′ (Figure 4b) and 6T Me (Figure 4d, cross-peak 12) agree with a *major groove* position close to the 5′-side nucleotide's sugar C2′ substituents. In contrast, the 5A H8 intense cross-peak with the attached sugar's H1′ (Figure 4b, cross-peak 7) and moderate cross-peaks with 4A H2 (Figure 4a, cross-peak 3) and bizelesin indole subunit's H3′ and H5′ (Figure 4a, cross-peaks 4 and 2, respectively) indicate a *minor groove* location close to the 5A sugar's C1′ position.

Disrupted H-Bonding of the AT Step of the 5OP Product Is Revealed by Loss of the Imino-to-Imino Cross-Peak. While an intense imino-to-imino cross-peak links *5HG* 7T H3 (4A-7T) to neighboring 6T H3 (5A-6T), no corresponding cross-peak was found for *5OP* 17T H3 (14.23 ppm; 14A-17T) and any signal in the chemical shift range (11–15 ppm) expected for 16T H3. The *5HG* 6T H3 signal's downfield chemical shift, sharpness, and intense cross-peak with 5A H8 support hydrogen bonding via N7 with 6T H3 and Hoogsteen base pairing (Figure2, cross-peak E1). All nonterminal base imino signals for *5HG* and *5OP* produce the expected set of NOESY (H_2O) cross-peaks (Figure 2, cross-peaks of signals A–F and H) except 16T H3 which was undetectable. The atypical behavior of 16T H3 and especially the lack of a detectable 17T H3 imino-to-imino cross-peak suggest disrupted hydrogen bonding for the two internal base pairs (5′-15A-16T-3′ with 3′-16T-15A-5′).

The AT Step of 5OP Is Characterized by Three Thymine Positional Isomers Indicated by Conformational Exchange. The *5OP* NOESY cross-connectivity network includes a primary set of "a" signals (conformer a) as well as additional "b" and "c" signals (conformers b and c) associated with the 16T region. Intense 200-ms NOESY exchange cross-peaks link a 16T methyl signal at 1.09 ppm (16Ta) to two smaller methyl signals at 0.88 ppm (16Tb) and 0.70 ppm (16Tc) (Figure 5). The 16Tb methyl signal produces a cross-peak with the adjacent 17Tb methyl (1.49 ppm), and the 16Tc methyl shares a cross-peak with the 17Tc methyl signal that partially overlaps the larger 17Ta methyl signal. An intense exchange cross-peak links the overlapped 17Ta and 17Tc methyl signals with the 17Tb methyl signal. Conformer b and c 16T methyl signals display cross-connectivity to corresponding 16T H6 signals. These H6 signals plus the methyl signals represent the total detectable signals of the minor b and c conformers that differ appreciably in chemical shift from the corresponding signals of the a conformer.

ROESY "negative" (ROESY conformational exchange cross-peaks have an opposite sign from dipolar cross-peaks) thymine H6 × H6 and Me × Me cross-peaks indicate that the three conformers are interconverting on the NMR time scale (0.2 s) and that the only significant difference between them is the position of the 16T base. 16T Me and H6 chemical shifts for the a, b, and c conformers suggest that they differ by the position of this base, which is freer to move than a normally base-paired thymine. Little difference between non-16T base signals for these three conformers suggests that 15A-16T base-pair opening causes only minor perturbation of neighboring base pairs.

Structures of 5HG and 5OP Generated by Restrained Molecular Dynamics. The model structures resulting from preliminary restrained molecular dynamics calculations (172 NMR distance constraints for *5HG*, Figure 6a; 189 NMR distance constraints for *5OP*, Figure 6b) are included to aid in visualizing the two adduct models. (In order to further refine structural differences beyond the major features described here, a detailed discussion of rMD results for *5HG* and *5OP* will follow in a subsequent publication.)

DISCUSSION

^1H NMR analysis of the bizelesin adduct of d(CGTAATTACG)$_2$ reveals that the central duplex region, 5′-TAATTA-3′, is cross-linked, yielding two major adduct conformations: one (major product: 60%) contains a 5′-AT-3′-step wherein both adenines are *syn*-oriented and Hoogsteen base paired to thymines (*5HG* model); the other contains *anti*-oriented AT-step adenines that show no evidence of hydrogen bonding with pairing thymines (*5OP* model; 40%).

NOESY Data Indicate That C_2 Symmetry of the Unmodified Duplex Is Preserved in 5HG and 5OP Structures. Division of the signals in the NOESY spectra into two cross-connectivity networks can be explained by two possible scenarios: (1) the product is a mixture of different conformers or (2) the product is a single structure in which each duplex strand produces a distinct cross-peak network. In the first case, the spectrum would contain two or more sets of entirely independent signals (no NOESY cross-peak links signals of different sets). In the second case, interstrand NOESY cross-peaks would link signals of the strand 1 set with signals of the strand 2 set. Results from the present study indicate that all interstrand NOESY cross-peaks occur between members of the same cross-connectivity network. For example, interstrand cross-peaks link 4A H2 with 8A H2 and H1′, 8A H2 with 4A H1′, 14A H2 with 18A H1′, 15A H2 with 17T H1′, and 18A H2 with 14A H2 and H1′. Although bizelesin produces

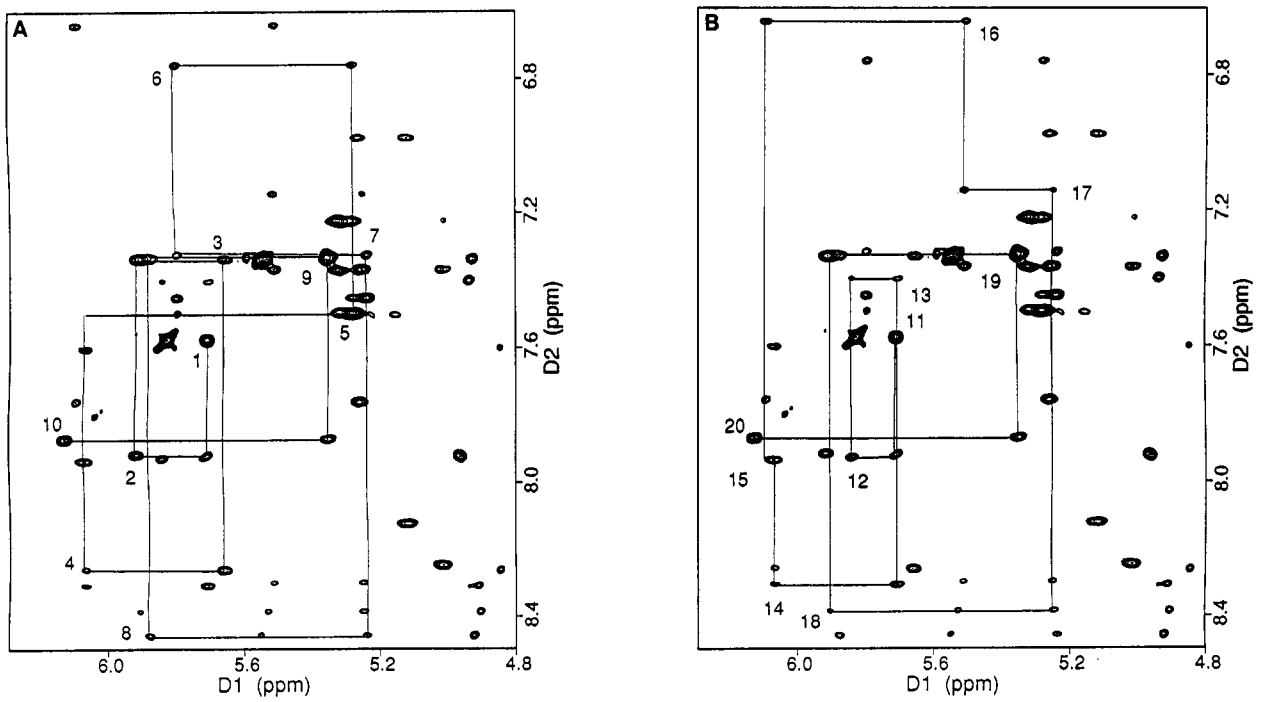

FIGURE 3: Two-dimensional phase-sensitive NOESY (200-ms mixing time) expanded contour plot of the bizelesin 10-mer duplex adduct in buffered D_2O solution, pH 6.85, at 23 °C displaying connectivities for PuH8/PyH6 to sugar H1′ (labeled with base number) and PuH8/PyH6 to sugar H1′ protons of the 5′-neighbor: A, *5HG* walk (1C to 10G); B, *5OP* walk (10C to 20G).

numerous NOESY cross-peaks with both duplex strands, cross-peaks link each of the two sets of drug ^{1}H signals with DNA ^{1}H signals of only one duplex cross-connectivity network.

Except for the instances of conformational exchange described above, only one set of ^{1}H signals characterizes each cross-connectivity network. Absence of any cross-peaks linking proton signals of these two networks indicates that the C_2 symmetry of the unmodified 10-mer duplex is preserved in each product, *5HG* and *5OP*.

Asymmetry of 5HG 5A Purine about the Glycosidic Bond Permits Unambiguous Assignment of HG Stereochemistry in 5HG. ^{1}H NOESY cross-peak data confirm that the *5HG* central 5′-AT-3′-step consists of HG base pairs stacked between flanking WC base pairs in right-handed DNA. Stereoviews of the AT-step region (Figure 6a for *5HG*) include numbered dashed lines that correspond to moderate or intense cross-peaks (Figure 4). The most diagnostic ^{1}H cross-peaks differentiating HG from WC pairing are those associated with adenine H2 and H8 and thymine H3. *Anti* to *syn* rotation moves H2 to a major groove environment similar to that occupied by H8 previous to rotation and relocates H8 into the minor groove. However, purine asymmetry about the glycosidic bond (C1′–N9) axis of rotation causes H2 (*syn*) to be driven to a position farther along the periphery of the major groove than occupied by H8 previous to rotation (*anti*). After rotation, H8 (*syn*) projects a correspondingly shorter distance into the minor groove than prerotation H2 (*anti*).

Differentiation of HG and WC ^{1}H NMR signals depends on this asymmetry. An intense 5A H8 × H1′ (intranucleotide) NOESY cross-peak (Figure 4b, cross-peak 7, and Figure 6a) corresponds in intensity to the distance from H1′ to *syn*-H8 (approximately 2.5 Å) instead of *anti*-H8 (approximately 3.9 Å). *Syn*-5A H2 intense cross-peaks with 5′-side 4A H8, H2″, and H2′ (Figure 4a, cross-peak 1; Figure 4c, cross-peaks 10 and 11, respectively) indicate greater base–base stacking of 4A and 5A than would be possible with *anti*-oriented 5A. Modeling predicts that the stacking of *anti*-4A and *syn*-5A positions the 3′-side (6T) thymine's methyl group in the maximal shielding zone of the 5A ring current effect (Figure 6). The remarkable chemical shift of this methyl group (0.60 ppm, Figure 5) supports this prediction. Proper base–base stacking and minimal deformation of the duplex structure in this region position the 5A N7 close to the H3 of the pairing thymine (6T). An intense 6T H3 × 5A H8 cross-peak (Figure 2, E1) and 6T H3 downfield chemical shift (12.38 ppm) indicate hydrogen bonding between 5A N7 and 6T H3. Further, an intense NOESY (H_2O) 7T H3 × 6T H3 cross-peak suggests a properly base-paired and stacked region.

Disrupted Hydrogen Bonding and Mobile AT-Step Thymine Bases Indicate 5OP Pairing Anomalies. Although ^{1}H NOESY data show that the *5OP* AT-step bases are *anti*-oriented (e.g., cross-peaks 8 and 9 between 15A H2 and 16T H1′ and 17T H1′, respectively; Figures 6b and 4), their open state (disrupted hydrogen bonding) is expressed by two lines of evidence: (1) Typically, duplex thymine H3 imino signals (NOESY in H_2O) occur between 12.0 and 15.0 ppm, due to the hydrogen bonding of base-paired thymine H3 (Figure 2). However in *5OP*, the 16T H3 signal is undetectable in the 10.0–15.0 ppm range, presumably due to disruption of hydrogen bonding. (2) NOESY and ROESY conformational exchange cross-peaks (Choe et al., 1991) indicate three AT-step thymine positional isomers. The extraordinarily different 16T methyl and H6 chemical shifts of conformers a, b, and c are evidence for 16T bases that are freer to move than a hydrogen-bonded thymine. Little difference between non-16T signals for these three conformers suggests that 15A-16T base-pair opening causes only minor perturbation of neighboring base pairs, which is consistent with proposed models for base-pair opening (Ramstein & Lavery, 1988). The exchange pathways and thymine chemical shift differences suggest that the 16T thymine isomers arise from the rotating motion about the glycosidic bond axis (Figure 5). As no direct 16Tb ↔ 16Tc exchange cross-peaks were detected, rotation proceeds predominantly in opposite directions from the central 16Ta position to give either conformer b or conformer c. Presumably, influence of adjacent duplex and/or drug moieties

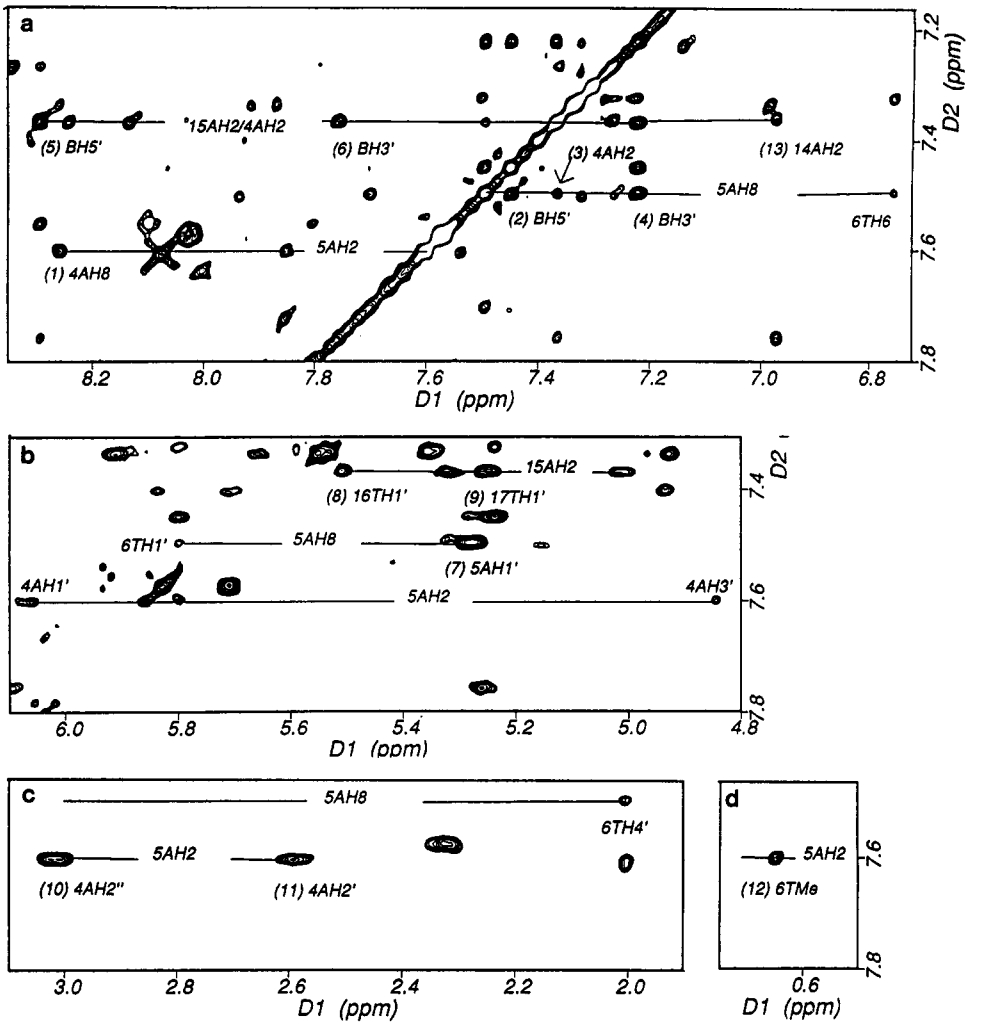

FIGURE 4: 2D NOESY (100-ms) expansions showing cross-peaks of 5A and 15A adenine H2 and H8 signals with (a) other aromatic protons, (b) sugar H1′ and H3′ protons, (c) sugar H2″ and H2′, and (d) thymine methyl protons. *5HG* numbering follows a 5′ to 3′ direction from 1 to 10 for both strands; *5OP* numbering proceeds from 11 to 20 for both strands. Numbers in parentheses refer to ^{1}H contacts shown in Figure 6.

suspends this motion long enough to "freeze out" conformers b and c. As the neighboring entities are also mobile, the influence is temporary, allowing for continued exchange between conformer a and the two minor b and c conformers.

Minor Groove Interactions of Bizelesin: 5HG vs 5OP Structures. *Syn* orientation of both *5HG* AT-step adenines deepens the minor groove in the region where the drug pivots about the ureadiyl moiety (Figure 6a). This depth difference is evident in the bizelesin 8H5′ and H9′ contacts with the duplex: *5HG* ureadiyl 8NH9′ (8.64 ppm) displays a pair of relatively intense cross-peaks with 6T H1′ and 8H5′ (7.45 ppm). 18NH9′ (7.66 ppm) shows cross-peaks with 15A H2 (strong), 16T H1′ (moderate), and 18H5′ (weak; 8.28 ppm). These cross-peaks suggest that 18NH9′ is closer to the *anti*-oriented 15A H2 than to the 18H5′ of the adjacent indole moiety, while 8NH9′ is closer to 8H5′ than to the relatively more distant *syn*-oriented 5A H8. Thus, the most intense 8H9′ cross-peak is with 8H5′ (intradrug), while the most intense 18H9′ cross-peak is with 15A H2 (drug to DNA).

The Changing Role of Bizelesin during Cross-Linkage of 5′-TAATTA-3′. Bizelesin's insertion into the minor groove provides the impetus for the joint reorientation of the *5HG* 5′-AT-3′ adenines, and the resulting HG base pairs are "locked" into place upon completion of cross-linkage. An explanation of this apparent paradox of adenine rotational freedom and reduced duplex flexibility is that while initial drug insertion assists isomerization of the adenines, the cross-linking reaction begins to exert a negative influence as covalent bond formation reduces the flexibility of the central duplex region. Inflexibility of the cross-linked DNA denies adenine its full arc of rotation, trapping duplex conformers that have adopted predominantly *syn* orientations in the AT-step region.

Adenine *anti* to *syn* reorientation swings this base's six-membered ring through the region of either the 5′-side adenine (4A) or 3′-side thymine (6T). The *5OP* conformer's 16T conformational exchange data suggest that *5HG*'s corresponding 3′-side thymine (6T) is less likely than 4A adenine to block 5A adenine's rotational arc. This 3′-side rotation requires that the base pairing (hydrogen bonding) of the rotating adenine and of the 3′-side thymine be simultaneously open when the base flips from *anti* to *syn* orientation. Under bizelesin's influence, *5HG* 6T thymine in the open state (previous to adenine rotation) presumably adopts a motion similar to that described above for *5OP* 16T thymine.

Although bizelesin's migration toward the floor of the minor groove and contact with neighboring bases influence *5HG* formation, the extent to which drug insertion drives adenine rotation is difficult to assess. The *5OP* conformer's behavior confirms that bizelesin is capable of shifting AT-step base-pair opening rates to give apparently permanent open states. Thus, drug insertion-induced base-pair opening, which is a prerequisite for base reorientation, is controlled by the drug.

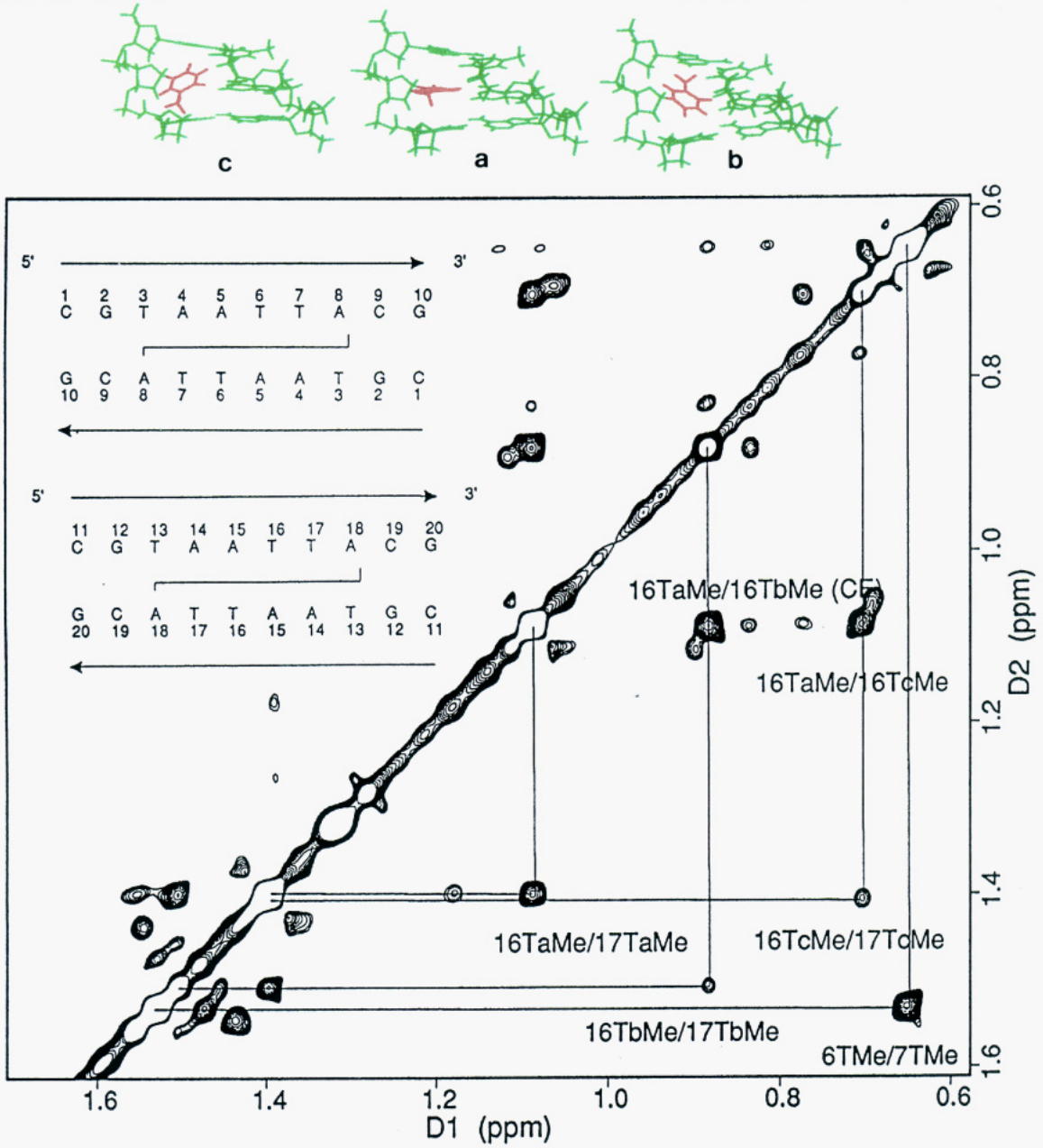

FIGURE 5: Two-dimensional NOESY (200-ms mixing time) expanded contour plot of the bizelesin 10-mer duplex adduct showing the *5HG* 6T and 7T and *5OP* 16T and 17T methyl-to-methyl internucleotide cross-peaks and direct conformational exchange cross-peaks. 16T thymine (red) is shown in the three positions suggested by conformational exchange cross-peaks.

However, the extent of the control by the drug of subsequent adenine rotation is unclear. Unquestionably, the *5HG* rotation product is a stable duplex answer to the steric stress associated with cross-linkage.

Absence from the products of an AT-step OP/HG mixed conformer indicates that the only two 5′-AT-3′ structures are OP/OP and HG/HG. The implication of the experimental results is that the OP/HG isomer either is a short-lived, relatively unstable intermediate or is not an intermediate, and the HG/HG isomer is produced directly by the concerted *anti* to *syn* rotation of both AT-step adenines. In either case, the results portray a central 5′-AATT-3′ region wherein the amplitude of motion is sufficiently broad to permit both adenines to rotate through a 180° arc despite the presence of flanking bases.

Bizelesin's Generation of a Stable Hoogsteen Base-Pairing Region in Otherwise "Normal" B-Form DNA Affords an Unprecedented Opportunity for Analysis of This Mode of Base Pairing. The chief obstacle to HG base-pairing analysis is the low probability that base pairs will undergo WC to HG transition, due to the high-energy barrier associated with base rotation. In order to induce formation of a significant concentration of Hoogsteen base-paired product, a drug must (1) extract the rarely formed HG isomer from the equilibrium WC/HG mixture, (2) stabilize the conformer by blocking *syn* to *anti* counterrotation, and (3) avoid radically distorting DNA structure in the WC-to-HG-to-WC transition region. Quinoxaline intercalators, triostin-A (Wang et al., 1984, 1986) and echinomycin (Mendal & Dervan, 1987; Gao & Patel, 1988; Gilbert et al., 1989), partially stabilize HG base pairs formed to the 3′-side of intercalation. For example, in the octamer $d(ACGTACGT)_2$ echinomycin produces stable HG terminal AT base pairs, but HG internal AT base pairs begin exchanging with open or WC base pairs as physiological temperatures are approached. Unfortunately, intercalator insertion disrupts base stacking and base–backbone interactions in the HG base-pair region. In contrast, bizelesin does not intrude into the base stacking of the WC to HG base-pair

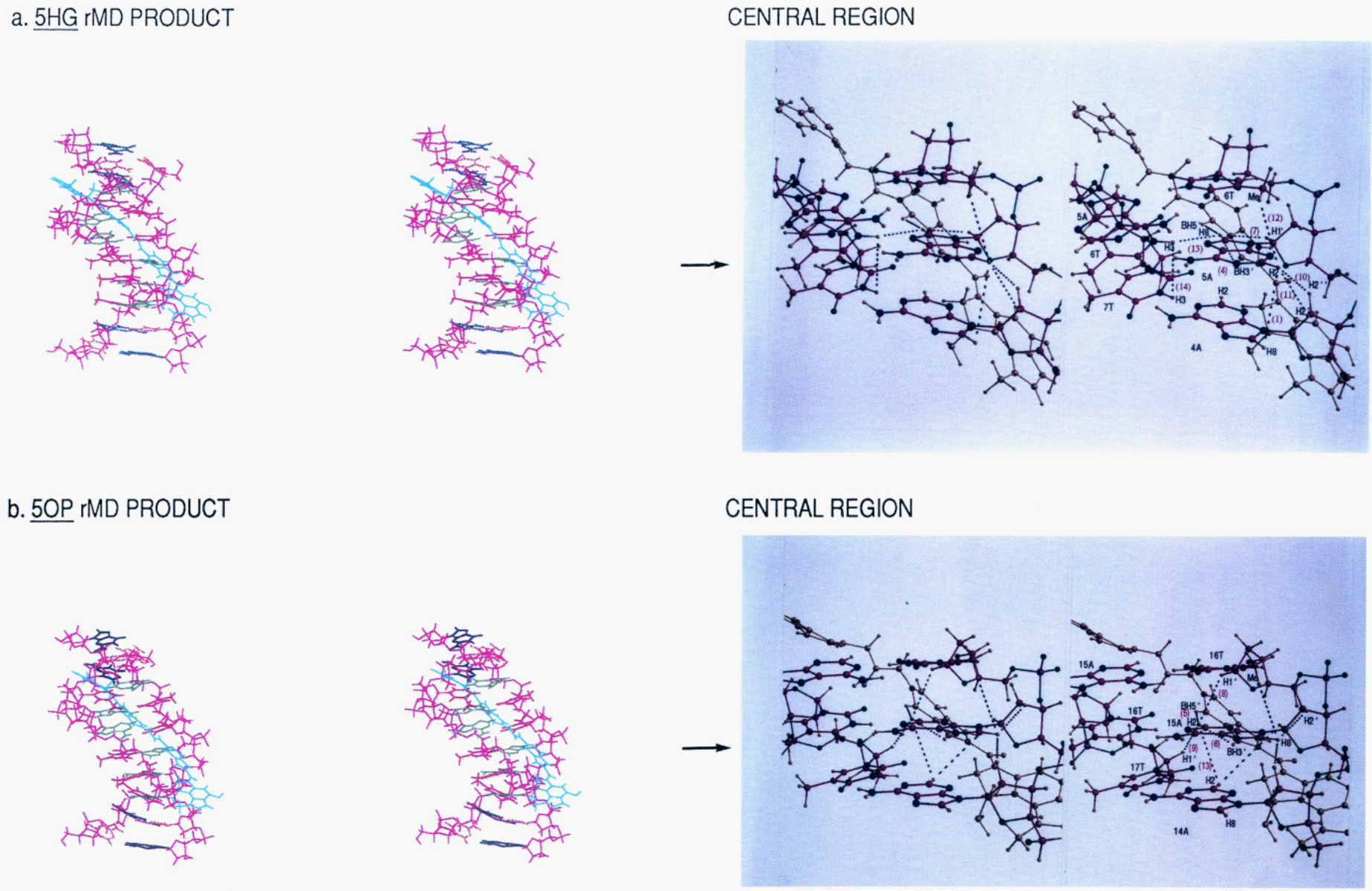

FIGURE 6: Model structure stereoviews of (a) *5HG* and (b) *5OP* restrained molecular dynamics products for the bizelesin adduct of the d(CGTAATTACG)$_2$ duplex and central regions showing moderate to intense NOESY cross-peaks (dashed lines) observed for nonexchangeable and exchangeable protons. Colors: (full adduct) magenta, DNA backbone; green, adenine; blue, guanine; red-yellow stripe, cytosine; red, thymine; cyan, bizelesin; (central region) solid yellow structure in minor groove, bizelesin. Number on dashed lines corresponds to cross-peak numbers in parentheses in Figure 4.

transition region and yields internal AT base pairs that are temperature stable.

ACKNOWLEDGMENT

We are grateful to David Bishop for editorial assistance and preparation of the manuscript.

REFERENCES

Bax, A., & Sarkar, S. K. (1984) *J. Magn. Reson. 60*, 170–176.
Blake, P. R., & Summers, M. F. (1990) *J. Magn. Reson. 86*, 622–625.
Borgias, B. A., & James, T. L. (1988) *J. Magn. Reson. 79*, 493–512.
Borgias, B. A., & James, T. L. (1990) *J. Magn. Reson. 87*, 475–487.
Borgias, B. A., Thomas, P. D., & James, T. L. (1987, 1989) *Complete Relaxation Analysis (CORMA)*, University of California, San Francisco.
Borgias, B. A., Gochin, M., Kerwood, D. J., & James, T. L. (1990) *Prog. Nucl. Magn. Reson. Spectrosc. 22*, 83–100.
Bothner-By, A. A., Stevens, R. L., Lee, J. T., Warren, C. D., & Jeanloz, R. W. (1984) *J. Am. Chem. Soc. 106*, 811–813.
Choe, B., Cook, G. W., & Krishna, N. R. (1991) *J. Magn. Reson. 94*, 387–391.
Ding, Z.-M., & Hurley, L. H. (1991) *Anti-Cancer Drug Des. 6*, 427–452.
Feigon, J., Rajagopal, P., & Gilbert, D. (1990) *UCLA Symp. Mol. Cell. Biol., New Ser. 109*, 249–258.
Gait, M. J., Ed. (1984) *Oligonucleotide Synthesis—A Practical Approach*, IRL Press, Oxford, England.
Gao, X., & Patel, D. (1988) *Biochemistry 27*, 1744–1751.
Gilbert, D. A., van der Marel, G., van Boom, J. H., & Feigon, J. (1989) *Proc. Natl. Acad. Sci. U.S.A. 86*, 3006–3010.
Hanka, L. J., Dietz, A., Gerpheide, S. A., Kuentzel, S. L., & Martin, D. G. (1978) *J. Antibiot. 31*, 1211–1217.
Hoogsteen, K. (1959) *Acta Crystallogr. 12*, 822–823.
Kerwood, D. J., Zon, G., & James, T. L. (1991) *Eur. J. Biochem. 197*, 583–595.
Lane, A. N., Jenkins, T. C., Brown, T., & Neidle, S. (1991) *Biochemistry 30*, 1372–1385.
Leroy, J.-L., Charretier, E., Kochoyan, M., & Guéron, M. (1988) *Biochemistry 27*, 8894–8898.
Lin, C. H., Beale, J. M., & Hurley, L. H. (1991) *Biochemistry 30*, 3597–3602.
Mendel, D., & Dervan, P. B. (1987) *Proc. Natl. Acad. Sci. U.S.A. 84*, 910–914.
Mitchell, M. A., Kelly, R. C., Wicnienski, N. A., Hatzenbuhler, N. T., Williams, M. G., Petzold, G. L., Slightom, J. L., & Siemieniak, D. R. (1991) *J. Am. Chem. Soc. 113*, 8994–8995.
Moe, J. G., & Russu, I. M. (1990) *Nucleic Acids Res. 18*, 821–827.
Nerdal, W., Hare, D. R., & Reid, B. R. (1989) *Biochemistry 28*, 10008–10021.
Pearlman, D. A., Case, D. A., Caldwell, J., Seibel, G. L., Singh, U. C., Weiner, P. K., & Kollman, P. A. (1991) *AMBER 4.0 (UCSF)*, University of California, San Francisco.
Ramstein, J., & Lavery, R. (1988) *Proc. Natl. Acad. Sci. U.S.A. 85*, 7231–7235.
Sarai, A., Mazur, J., Nussinov, R., & Jernigan, R. L. (1989) *Biochemistry 28*, 7842–7849.
Searle, M., & Wickham, G. (1990) *FEBS Lett. 272*, 171–174.
Singh, U. C., Pattabiraman, N., Langridge, R., & Kollman, P. A. (1986) *Proc. Natl. Acad. Sci. U.S.A. 83*, 6402–6406.
Sklenar, V., & Bax, A. (1987) *J. Magn. Reson. 74*, 469–479.
Sun, D., & Hurley, L. H. (1993) *J. Am. Chem. Soc. 115*, 5925–5933.
Wang, A. H.-J., Ughetto, G., Quigley, G. J., Hakoshima, T., van der Marel, G., van Boom, J. H., & Rich, A. (1984) *Science 225*, 1115–1121.
Wang, A. H.-J., Ughetto, G., Quigley, G. J., & Rich, A. (1986) *J. Biomol. Struct. Dyn. 4*, 319–342.